7. Tasaki K, Shima T, Nishida M, Yamada T, Nishida T. Spontaneous disappearance of arteriovenous malformation in angiogram–an operated case. *Jpn J Stroke* 1990;12:40–46.
8. Ezura M, Kagawa S. Spontaneous disappearance of a huge cerebral arteriovenous malformation: case report. *Neurosurgery* 1992;30:595–599.
9. Tyler JL, Leblanc R, Meyer E, et al. Hemodynamic and metabolic effects of cerebral arteriovenous malformations studied by positron emission tomography. *Stroke* 1989; 20:890–898.
10. De Reuck J, Van Aken L, Van Landegem W, Vakaet A. Positron emission tomography studies of changes in cerebral blood flow and oxygen metabolism in arteriovenous malformation of the brain. *Eur Neurol* 1989;29:294–297.
11. Sayama I, Mizuno M, Yasui N, Kanno I, Shishido F. Regional evaluation of cerebral hemodynamics and metabolism in the arterio-venous malformation using positron emission tomography. *Surgery for Cerebral Stroke (Jpn)* 1990;18:303–308.
12. Fink GR. Effects of cerebral angiomas on perifocal and remote tissue: a multivariate positron emission tomography study. *Stroke* 1992;23:1099–1105.
13. De Reuck J, De La Meilleure G, Boon P, et al. Comparison of cerebral hemodynamic and oxygen metabolic changes due to cavernous angiomas and arteriovenous malformations of the brain–a positron emission tomography study. *Acta Neurol Belg* 1994;94:239–244.
14. MG Yasargil. Special surgical considerations. In: Yasargil MG, ed. *Microneurosurgery 3B AVM of the brain, clinical considerations, surgical and special operative techniques, surgical results, nonoperated cases, cavernous and venous angiomas, neuroanesthesia.* Stuttgart: Georg Thieme Verlag; 1988:55–368.
15. Spetzler RF, Martin NA. A proposed grading system for arteriovenous malformations. *J Neurosurg* 1986;65:476–483.
16. Frackowiak RS, Lenzi GL, Jones T, Heather JD. Quantitative measurement of cerebral blood flow and oxygen metabolism in man using ^{15}O and positron emission tomography: theory, procedure and normal values. *J Comput Assist Tomogr* 1980;4: 727–736.
17. Phelps ME, Huang S-C, Hoffman EJ, Kuhl DE. Validation of tomographic measurement of cerebral blood volume with ^{11}C-labeled carboxyhemoglobin. *J Nucl Med* 1979;20:328–334.
18. Grubb RL, Raichle ME, Higgins CS, Eichling JO. Measurement of regional cerebral blood volume by emission tomography. *Ann Neurol* 1978;4:322–328.
19. Lammertsma AA, Jones T. Correction for the presence of intravascular oxygen-15 in the steady-state technique for measuring regional oxygen extraction ratio in the brain: 1. Description of the method. *J Cereb Blood Flow Metab* 1983;3:416–424.
20. Jones T, Chesler DA, Ter-Pogossian MM. The continuous inhalation of oxygen-15 for assessing regional oxygen extraction in the brain of man. *Br J Radiol* 1976;49:339–343.
21. Gibbs JN, Wise RJ, Leenders KL, Jones T. Evaluation of cerebral perfusion reserve in patients with carotid artery occlusion. *Lancet* 1984;1:310–314.
22. Gibbs JN, Wise RJ, Leenders KL, Herold S, Frackowiak RS, Jones T. Cerebral hemodynamics in occlusive carotid artery disease. *Lancet* 1985;1:933–934.

Extensive Photopenic Osteomyelitis

Patrice K. Rehm and Alan D. Aaron
Division of Nuclear Medicine, Departments of Radiology and Orthopedic Surgery, Georgetown University Hospital, Washington, D.C.

We present a case of a previously healthy child whose osteomyelitis and septic arthritis resulted in unusually extensive photopenia on bone scintigraphy. Uptake was absent in the humeral shaft and proximal epiphysis and decreased in the proximal physis. The subsequent complicated clinical course, including surgical interventions, and bone scans is described.

Key Words: bone scintigraphy; photopenic osteomyelitis; septic arthritis

J Nucl Med 1996; 37:1676–1678

CASE REPORT

The morning of hospitalization, a previously healthy 3-yr-old girl presented to her pediatrician for pain in her left upper arm. Evaluation revealed an afebrile child with mild tenderness in her upper arm and multiple healing insect bites on her extremities. Her white blood cell count was 8800 per mm^3, with 46% polymorphonuclear cells and 34% bands. The erythrocyte sedimentation rate was 6 mm/hr. Radiographs of the left humerus were normal. The patient was begun on oral penicillin and ampicillin to treat cellulitis.

Within 24 hr, the child became febrile to 105 degrees and confused, requiring hospitalization and administration of intravenous nafcillin. Over the next 12 hr, the arm became increasingly swollen and erythematous, with eventual extension to the anterior shoulder and chest wall. Numerous petechia appeared on her trunk and lower extremities. A ^{99m}Tc-HDP bone scan demonstrated extensive photopenia of the left humerus (Fig. 1).

Based on a clinical diagnosis of septic arthritis of the shoulder and osteomyelitis of the adjacent humeral metaphysis, the patient was taken emergently to the operating room for exploration and debridement. At surgery, purulent material was found within the glenohumeral joint, with the humerus being free of obvious infection. Intraoperative gram stain and cultures revealed *S. aureus*.

Intravenous nafcillin was continued, but on the fifth hospital day, the patient remained febrile necessitating surgical re-exploration. Reaccumulation of purulent material was found in the glenohumeral joint, with additional purulence within the proximal humeral metaphysis, neither being under pressure. Two days after the second surgery, radiographs revealed periosteal reaction (Fig. 2A), while bone scintigraphy again demonstrated photopenia (Figs. 2B, C).

A third bone scan on Day 18 revealed increased activity throughout most of the humerus (Figs. 2D, E). Pretreatment and multiple subsequent blood cultures as well as cardiac echo were normal. The child defervesced and was treated with intravenous gentamicin and nafcillin for 6 wk.

At 9 wk, she presented with a pathological fracture of the

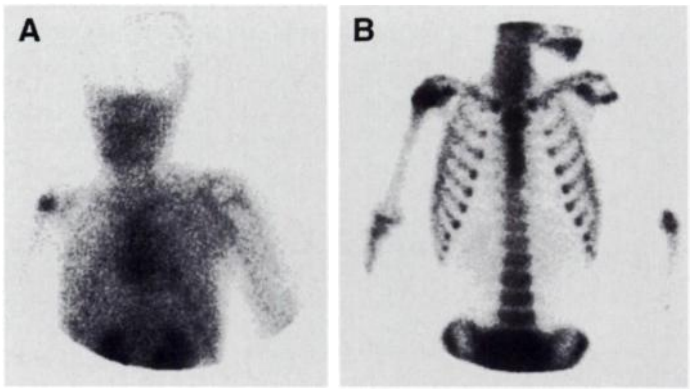

FIGURE 1. (A) Blood-pool image demonstrates relative photopenia of the left proximal epiphysis and humeral shaft, with a sleeve of increased activity around the nonvisualized shaft. (B) Delayed image demonstrates absent uptake in the entire humeral shaft and the proximal epiphysis and reduced uptake in the proximal physis. The distal metaphysis, although not optimally demonstrated, shows increased uptake.

Received May 19, 1995; revision accepted Jan. 24, 1996.
For correspondence or reprints contact: Patrice K. Rehm, MD, Division of Nuclear Medicine, Gorman 2005, Georgetown University Hospital, 3800 Reservoir Rd. NW, Washington, D.C. 20007-2113.

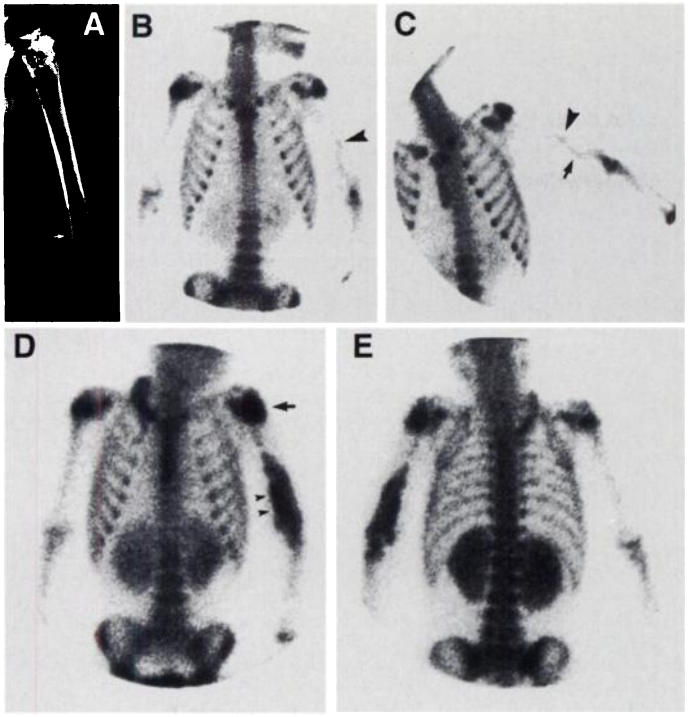

FIGURE 2. (A) Radiograph of the left humerus demonstrates minimal periosteal reaction (arrow). Postoperative bone defects and gas in the soft tissues are present. (B) Anterior and (C) oblique delayed views demonstrate absent uptake in the left humeral shaft except for a small focus in the midshaft (arrowhead). Linear radiotracer (arrow) outside the expected humeral contour represents activity in elevated periosteum. There is improved but persistently decreased uptake in the proximal physis. (D) Anterior and (E) posterior delayed images demonstrate increased activity in the proximal physis and epiphysis (arrow); radiotracer intensity obscures their distinction. Distally increased activity extends beyond the expected cortex (arrowheads), indicating exuberant periosteal reaction. A short segment of the diaphysis remains photopenic. There is radiotracer retention in the central intravenous line used for injection.

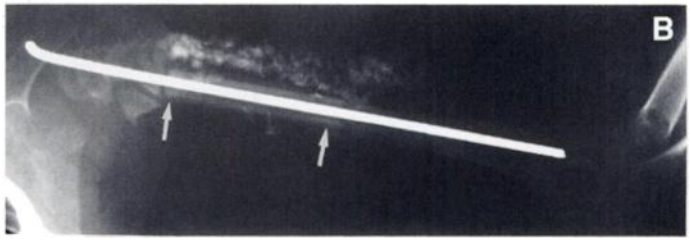

FIGURE 3. (A) There is diffuse osteolysis of the humerus and fragmentation of the proximal epiphysis and metaphysis. An involucrum and two pathological fractures (arrows) are present. (B) Postoperative scan demonstrates an intramedullary rod and bone graft, including a fibular autograft (arrows).

proximal humerus (Fig. 3A). The patient subsequently developed an atrophic nonunion, necessitating surgical stabilization with an intramedullary rod and a vascularized fibular autograft (Fig. 3B).

DISCUSSION

Acute hematogenous osteomyelitis is most often demonstrated on delayed bone scan images as increased radiotracer, although normal (*1*) and photopenic or "cold" patterns (*2,3*) have been described. The extent of the initial scintigraphic findings prompted our review of the literature, which revealed 35 cases of photopenic osteomyelitis in children (without sickle cell disease) involving long bones (*3–18*), the head of the femur (*12,19–21*) or humerus (*22*), ilium (*20,23*), ischium (*12,19–21*), talus (*24*) and patella (*14*). Segmental photopenia involving the metaphysis has been reported most frequently, with or without adjacent increased activity. Large photopenic regions have been described less commonly (*8,20,21*). Typically, the initial photopenic area shows increased activity on subsequent scans (*3,25*).

As in this case, *S. aureus*, the most common cause of osteomyelitis in children outside the neonatal period, was identified in nearly all those reporting bacteria.

Based on the pathophysiology of acute osteomyelitis in children (*26*), the initial infection starts in a juxta-metaphyseal vascular loop, where ramifications of the nutrient artery turn sharply at the growth plate which is not penetrated between 1 yr of age and puberty. The combination of vascular anatomy, sluggish blood flow in sinusoidal veins and absence of functionally active phagocytes predisposes the metaphysis to infection. Initial hyperemia and edema result in a rise in marrow cavity pressure. The microvasculature may become occluded through compression, thrombosis or both. The resulting decreased delivery of blood and tracer to the area may result in a normal or photopenic appearance. The infrequent demonstration of photopenia suggests that the scan has been obtained after the early phase of infection (*27*).

Subperiosteal or intraosseus pus, as was present at the second surgery, can lead to additional intraosseous pressure. The nutrient artery may be secondarily thrombosed or compromised as the infection spreads throughout the cortex, often leading to subperiosteal abscess formation. The infection may also cause septic thrombophlebitis of diaphyseal or medullary vessels (*26*). There are case reports documenting vascular occlusion (*3*) and others documenting patency of the large vessels (*21*). Areas of decreased uptake on delayed images have been attributed to areas of ischemic or devitalized bone (*10,12*). The increased activity on follow-up, as demonstrated in this case, has been attributed to osteoblastic activity in the periosteum, which remains vascularized (*3*), medullary decompression or ingrowth of new vessels from the elevated periosteum (*25*). "Stripes" of increased activity characteristic of revascularization from the periosteum can be present (*12*) (Figs. 2B, C).

In our patient, the osteomyelitis most likely originated in the proximal humeral metaphysis, which is intracapsular, and spread through a break in the cortex to involve the joint. This correlates with the scan abnormality being primarily humeral rather than articular. We postulate that the first scan, obtained within 24 hr of symptom onset, reflected the early phase. Persistent photopenia on the second scan likely reflected a combination of the pressure effects of intraosseous pus and ischemic or devitalized bone.

Decreased uptake in the proximal humeral epiphysis and physis can be explained by a variety of mechanisms. The intracapsular location of the proximal metaphysis of the humerus, like the femur, makes it particularly susceptible to

reductions in blood flow and tracer uptake secondary to either sterile or purulent intracapsular fluid (*12*). Blood flow and tracer uptake can be restored by reduction in the intracapsular pressure through aspiration or drainage (*28,29*). However, metaphyseal infection alone in the absence of joint effusion can compromise the blood flow to the head as edema and swelling of the overlying synovia compress the thin vessels that supply the head. While not present in this child, a subperiosteal abscess bulging into the joint can stretch and compress the epiphyseal arteries and veins within the synovia. Compromise of epiphyseal blood flow by any of these mechanisms may necessitate surgical drainage of the proximal humerus in addition to the glenohumeral joint (*22*).

Because no large series exists, inferences and conclusions regarding photopenic osteomyelitis must be based on case reports and selected series. Previous authors have noted an association between photopenia and subperiosteal (*6*) or intraosseous pus (*21*), thereby promoting the need for surgical drainage to decrease morbidity (*8*). Our review found this association in 25/35 reported cases. Computed tomography or MRI has been suggested to identify coexisting abscess in patients with photopenic osteomyelitis (*6*). Further evaluation of these modalities regarding patient outcome is warranted. However, in other reports where pus was absent, photopenia was presumed to be due to other pathophysiologic mechanisms.

Some authors have suggested that photopenia indicates a poor prognosis (*8*). As in this child, prolonged or complicated courses were noted in 10/35 reported cases in spite of aggressive management. The impairment of diaphyseal blood flow previously invoked to explain the massive sequestra seen before effective antibiotics (*30*) and decreased delivery of antibiotics may contribute to an increased risk for sequestrum formation and increased morbidity (*13*).

It is important not only to recognize photopenia as a manifestation of osteomyelitis but to alert the clinicians to vascular compromise and the frequent coexistence of intraosseous or subperiosteal abscesses. In this child, the initial bone scan, in addition to demonstrating the magnitude of the infection, documented that vascular compromise preceded and was not related to the subsequent surgical intervention. Persistent photopenia on the second scan, in conjunction with the lack of clinical improvement, contributed to the second surgical intervention which included the drainage of an intraosseous abscess. Therefore, appreciation of these factors may signal the need for more aggressive surgical management to decrease morbidity (*8,11*).

REFERENCES

1. Gilday DL, Paul DJ, Paterson J. Diagnosis of osteomyelitis in children by combined blood pool and bone imaging. *Radiology* 1975;117:331–335.
2. Handmaker H, Leonards R. The bone scan in inflammatory osseous disease. *Semin Nucl Med* 1976;6:95–105.
3. Russin LD, Staab EV. Unusual bone scan findings in acute osteomyelitis: case report. *J Nucl Med* 1976;17:617–619.
4. Rosovsky M, Goldfarb CR, Finestone H, Ongseng F. "Cold spots" in pediatric bone imaging. *Semin Nucl Med* 1994;24:184–186.
5. Grier D, Feinstein KA. Osteomyelitis in hospitalized children with chicken pox: imaging findings in four cases. *Am J Roentgenol* 1993;161:643–646.
6. Allwright SJ, Miller JH, Gilsanz V. Subperiosteal abscess in children: scintigraphic appearance. *Radiology* 1991;179:725–729.
7. Outwater E, Oates E, Sarno RC. Indium-111-labeled leukocyte scintigraphy: diagnosis of subperiosteal abscesses complicating osteomyelitis in a child. *J Nucl Med* 1988;29: 1871–1874.
8. Hamdan J, Asha M, Mallouh A, Usta H, Talab Y, Ahmad M. Technetium bone scintigraphy in the diagnosis of osteomyelitis in children. *Pediatr Infect Dis J* 1987;6:529–32.
9. Park HM, Rothschild PA, Kernek CB. Scintigraphic evaluation of extremity pain in children: its efficacy and pitfalls. *Am J Roentgenol* 1985;145:1079–1084.
10. Barron BJ, Dhekne RD. Cold osteomyelitis: radionuclide bone scan findings. *Clin Nucl Med* 1984;9:392–393.
11. Howie DW, Savage JP, Wilson TG, Paterson D. The technetium phosphate bone scan in the diagnosis of osteomyelitis in childhood. *J Bone Joint Surg [Am]* 1983;65:431–437.
12. Murray IP. Photopenia in skeletal scintigraphy of suspected bone and joint infection. *Clin Nucl Med* 1982;7:13–20.
13. Erasmie U, Hirsch G. Acute hematogenous osteomyelitis in children–the reliability of skeletal scintigraphy. *Z Kinderchir* 1981;32:360–366.
14. Jones DC, Cady RB. "Cold" bone scans in acute osteomyelitis. *J Bone Joint Surg [Br]* 1981;63:376–378.
15. Ash JM, Gilday DL. The futility of bone scanning in neonatal osteomyelitis: concise communication. *J Nucl Med* 1980;21:417–420.
16. Wald ER, Mirro R, Gartner JC. Pitfalls on the diagnosis of acute osteomyelitis by bone scan. *Clin Pediatr* 1980;19:597–601.
17. Lisbona, R, Rosenthall L. Observations of sequential use of ^{99m}Tc-phosphate complex and ^{67}Ga imaging in osteomyelitis, cellulitis and septic arthritis. *Radiology* 1977;123: 123–129.
18. Treves S, Khettry J, Broker FH, Wilkinson R, Watts H. Osteomyelitis: early scintigraphic detection in children. *Pediatrics* 1976;57:173–186.
19. Ang JG, Gelfand MJ. Decreased gallium uptake in acute hematogenous osteomyelitis. *Clin Nucl Med* 1983;8:301–303.
20. Teates CD, Williamson BRJ. "Hot and cold" bone lesions in acute osteomyelitis. *Am J Roentgenol* 1977;129:517–518. .
21. Trackler RT, Miller KE, Sutherland DH, Chadwick DL. Childhood pelvic osteomyelitis presenting as a "cold" lesion on bone scan: case report. *J Nucl Med* 1976;17: 620–622.
22. Mortensson W, Nybonde T. Ischemia of the childhood femoral and humeral head epiphyses following osteomyelitis: a hypothesis on its cause. *Acta Radiol [Diagn] (Stockh)* 1984;25:269–272.
23. Pijpers R, Ekkelkamp S, Roos JC, Teule GJ. Reduced perfusion and uptake of ^{99m}Tc-HDP in the iliac bone: a rare presentation of pelvic osteomyelitis. *Clin Nucl Med* 1994;19:516–518.
24. Majd M, Frankel RS. Radionuclide imaging in skeletal inflammatory and ischemic disease in children. *Am J Roentgenol* 1976;126:832–341.
25. Garnett ES, Cockshott WP, Jacobs J. Classical acute osteomyelitis with a negative bone scan. *Br J Radiol* 1977;50:757–760.
26. Waldvogel FA, Medoff G, Swartz MN. Osteomyelitis: a review of clinical features, therapeutic considerations and unusual aspects. *N Engl J Med* 1970;282:198–206.
27. Handmaker H. Acute hematogenous osteomyelitis: has the bone scan betrayed us? *Radiology* 1980;135:787–789.
28. Kloiber R, Pavlosky W, Portner O, et al. Bone scintigraphy of hip joint effusions in children. *Am J Roentgenol* 1983;140:995–998.
29. Wingstrand H, Egund N, Carlin NO. Intracapsular pressure in transient synovitis of the hip. *Acta Orthop Scand* 1985;56:204–210.
30. LeVeuf J. Treatment of osteomyelitis-anatomical and physiological basis. *J Bone Joint Surg* 1948;30B:2.